

Article

Influence of Addition of Fluid Catalytic Cracking Residue (FCC) and the SiO₂ Concentration in Alkali-Activated Ceramic Sanitary-Ware (CSW) Binders

Juan Cosa ¹, Lourdes Soriano ¹, María Victoria Borrachero ¹, Lucía Reig ² , Jordi Payá ¹ and José María Monzó ^{1,*} 

¹ ICITECH—Instituto de Ciencia y Tecnología del Hormigón, Grupo de Investigación en Química de los Materiales (GIQUIMA), Universitat Politècnica de València, 46022 Valencia, Spain; juacoma2@upv.es (J.C.); lousomar@upvnet.upv.es (L.S.); vborrhachero@cst.upv.es (M.V.B.); jjpaya@cst.upv.es (J.P.)

² EMC—Department of Mechanical Engineering and Construction, Universitat Jaume I, 12071 Castellón de la Plana, Spain; lreig@uji.es

* Correspondence: jmmonzo@cst.upv.es; Tel.: +34-963-877-564

Received: 7 March 2018; Accepted: 17 March 2018; Published: 21 March 2018



Abstract: Production of Portland cement requires a large volume of natural raw materials and releases huge amounts of CO₂ to the atmosphere. Lower environmental impact alternatives focus on alkali-activated cements. In this paper, fluid catalytic cracking residue (FCC) was used to partially replace (0 wt %–50 wt %) ceramic sanitaryware (CSW) in alkali-activated systems. Samples were activated with NaOH and sodium silicate solutions and were cured at 65 °C for 7 days and at 20 °C for 28 and 90 days. In order to increase CSW/FCC binders' sustainability, the influence of reducing the silica concentration (from 7.28 mol·kg⁻¹ up to 2.91 mol·kg⁻¹) was analyzed. The microstructure of the developed binders was investigated in pastes by X-ray diffraction, thermo tests and field emission scanning electron microscopy analyses. Compressive strength evolution was assessed in mortars. The results showed a synergetic effect of the CSW/FCC combinations so that, under the studied conditions, mechanical properties significantly improved when combining both waste materials (up to 70 MPa were achieved in the mortars containing 50 wt % FCC cured at room temperature for 90 days). Addition of FCC allowed CSW to be activated at room temperature, which significantly broadens the field of applications of alkali-activated CSW binders.

Keywords: sustainable construction materials; waste management; alkali-activated binder; fluid catalytic cracking; ceramic sanitaryware; mechanical strength; microstructure

1. Introduction

Portland cement is the most widely used construction material, which is attributed mainly to its availability, versatility, familiarity, relatively low cost, and the fact that its properties and durability have been widely investigated. According to the data provided by the U.S. Geological Survey [1], 4.2 billion tonnes of cement were produced worldwide in 2016 and, as reported by Imbabi et al. [2], this production is expected to increase and reach as much as 5.6 billion tonnes by 2050. The cement industry and the scientific community have been seeking alternatives to increase the sustainability of this basic construction material in an attempt to develop less harmful binders to the environment, with lower carbon emissions, that use fewer natural resources, and thus better contribute to a long-term ecologically balanced development. However, approximately 0.9 kg of CO₂ per kg of produced cement is released to the atmosphere [2], which implies that nearly 3.78 billion tonnes of CO₂ are generated

yearly (about 6% of global CO₂ emissions [2,3]). CO₂ emissions come mainly from the decomposition of limestone and clay raw materials, and from the energy used to achieve clinkering temperatures (close to 1450 °C).

The cement industry and the scientific community have explored different alternatives to improve Portland cement's sustainability. Some have focused on reducing emissions and the energy used during the production process [2]. Others, such as that by Puertas et al. [4,5], have used waste materials to produce clinker. Several studies have proved the suitability of different silicoaluminates by-products as pozzolanic admixtures to partially replace Portland cement [6–8]. Further studies have focused on developing new alternative low CO₂ binders, such as calcium sulfoaluminate cements [9] or alkali-activated binders [3]. As described in [10], an aluminosilicate material (precursor) is dissolved in alkaline media during the geopolymerization process, and Al and Si ions released as monomers polycondensate to form a new binder with an amorphous to semi-crystalline structure. As previously reported by Mellado et al. [11], the CO₂ emissions of the binders developed by the alkali-activation of spent fluid catalytic cracking residue (FCC), a by-product from the petrochemical industry, lowered by 13% when activated with NaOH and commercial waterglass solutions compared with PC mortars, and these emissions dropped by up to 63% when using alternative sources of silica (rice husk ash) in the activating solution. Aluminosilicate materials, such as blast furnace slag, metakaolin or fly ashes, have been widely used as precursors in alkali-activated systems [12–14]. However, in recent decades, different studies have investigated the suitability of other by-products, such as palm oil fuel ash [15], rice husk ash or red mud [16], as silicon and aluminum sources to develop new alkali-activated binders. Among them, the reutilization and valorization of ceramic materials is a very interesting research line to be explored given their prolonged biodegradation period (up to 4000 years) [17].

Ceramic sanitary-ware (CSW) waste (i.e., bidets, lavatories, washbasins, etc.) is a type of ceramic residue with high SiO₂ and Al₂O₃ contents (approximately 90%, some of which are in an amorphous state [17]) that has been successfully used as a precursor in [17,18]. According to Baraldi [19], approximately 349.3 million CSW units were produced worldwide in 2014, and Asia was the main producing region (49.2% of total production), followed by the European Union, where 41.6 million units were manufactured (11.9% of global production). As reported by Medina et al. [20], 5%–7% of the 7 million CSW pieces produced in Spain in 2008 were rejected for sale due to defects, such as cracks, nicks or glaze damage, or for technical considerations. Additionally, the CSW units deposited in dumps at the end of their life cycle can be easily separated since they are not generally adhered to other construction materials, such as gypsum or cement.

In a previous study, Reig et al. [18] successfully reused ceramic sanitary-ware waste as a precursor to produce alkali-activated binders. These authors observed that applying temperature during the curing process (65 °C) proved essential to activate CSW, and Ca(OH)₂ addition played an essential role in the fresh-state behavior of the developed CSW binders. The mix proportions of the activating solution were optimized so that compressive strength values of up to 36 MPa were achieved in the mortars cured at 65 °C for 7 days. Later studies [17] explored the influence of Ca(OH)₂, calcium aluminate cement (CAC) and Portland cement (PC) on the microstructure and mechanical properties of alkali-activated CSW. The obtained results decidedly increased the valorization possibilities of CSW as a precursor in alkali-activated binders, since the compressive strength results significantly improved with relatively low cement contents (64.41 and 70.69 MPa were achieved in the mortars blended with 10 wt % PC and 15 wt % CAC, respectively, cured at 65 °C for 7 days). According to the reported results [17], hydration of PC and CAC followed a different pathway from that generally observed in water, and the provided Ca and Al ions were taken up in the new alkali-activated binder to form (N,C)-A-S-H or C-A-S-H gels. Despite the mechanical properties significantly improving with PC or CAC additions, low CSW substitutions were recommended, because these cements use natural resources, release large volumes of CO₂ to the atmosphere and require huge amounts of energy to reach clinkering temperatures (close to 1450 and 1600 °C for PC and CAC, respectively) [17]. Thus, exploring if the partial substitution of CSW for some industrial by-product favors the activation of CSW at room

temperature, providing mechanical properties that allow these binders to be used in conventional construction applications, would contribute significant economic and environmental benefits. In line with this, spent fluid catalytic cracking residue (FCC) is a good candidate to be used. As explained by Trochez et al. [21], FCC is an aluminosilicate material with a zeolitic structure used to transform crude oil into fuel products by breaking long chains in hydrocarbon molecules. FCC is replaced when it loses its catalytic properties and is classified as inert waste. According to Trochez et al. [21], approximately 800,000 tons of this by-product are produced yearly worldwide.

Although FCC has been widely landfilled, in recent years, new alternatives for reusing and valorizing this waste have been explored. Among the uses related with cement and concrete industries, FCC has been successfully used in either Portland cement production [22] as a pozzolanic admixture [6,23–25], or in calcium aluminate systems [26]. The use of FCC as a precursor in alkali-activated binders has also been investigated in the last few years [21,27–29]. In the study by Tashima et al. [27], strength values within the 10–70 MPa range were obtained in mortars cured at 65 °C for 3 days, developed with a water/FCC ratio of 0.60 and activated with SiO₂/Na₂O ratios that ranged from 0 (no silica) to 1.46. Further research [28] analyzed the influence of different SiO₂/Na₂O and H₂O/FCC ratios on the mechanical properties and microstructure of alkali-activated FCC binders. The best results (68.3 MPa) were obtained for the mix prepared with 10 mol·kg^{−1} of Na and SiO₂/Na₂O and H₂O/Na₂O molar ratios of 1.17 and 11.11, respectively, and strength values further improved (up to 83.6 MPa) by reducing the water/FCC ratio from 0.60 to 0.45. The authors attributed the poorer performance of some mortars to a reduced alkalinity in the activating solution, which decreased the dissolution of the precursor and, consequently, the binder formation. Cheng et al. [30,31], who investigated the influence of FCC additions in alkali-activated metakaolin, established 10% as the optimum percentage of substitution. These authors also concluded that the SiO₂/Na₂O and solid/liquid ratios strongly determined the properties of the blended system.

This research aimed to investigate the influence of different FCC additions (0 wt %–50 wt %) and silica concentrations on the compressive strength and microstructure of alkali-activated ceramic sanitary-ware waste binders.

2. Materials and Methods

2.1. Materials

Ceramic sanitary-ware (CSW) units, rejected during the manufacturing process due to production defects, were supplied by the company Ideal Standard (Valencia, Spain). Pieces were produced following the process previously described by Medina et al. [20]: the prepared raw materials were cast into a mold which conferred the piece the desired shape; products were then dried to evaporate water and were finally sintered at temperatures within the 1200–1290 °C range. Units were broken into pieces with a hammer and crushed in a jaw crusher (BB200 Retsch) to reduce particle size to less than 2 mm. Crushed particles were then dry-milled in a Roller 1 jars turner roller by Gabrielli. Grinding was achieved by turning two cylindrical alumina 5 L volume jars for 6 h (190 rpm for the first 10 min and 140 rpm for the remaining time). Each jar was filled with 1500 g of ceramic waste and 6500 g of alumina balls. Fluid catalytic cracking catalyst residue (FCC) was supplied by the company Omya Clariana S.A. (Tarragona, Spain). The material was used as received.

Alkaline solutions were prepared by mixing sodium hydroxide pellets (98% purity, supplied by Panreac), water and waterglass (composed of 28% SiO₂, 8% Na₂O and 64% H₂O, supplied by Merck, Kenilworth, NJ, USA).

2.2. Experimental Flow Chart, Mix Proportions and Curing Conditions

The experimental process followed herein is summarized in Figure 1. Designation of samples, together with the mix proportions, concentrations, ratios of the activating solutions and curing conditions, are summarized in Table 1. In the first step of the study, the influence of different FCC

additions (0 wt %–50 wt %) on the CSW systems alkali-activated with a constant $\text{SiO}_2/\text{Na}_2\text{O}$ molar ratio (1.94, obtained with constant Na_2O and SiO_2 concentrations of 3.75 and $7.28 \text{ mol}\cdot\text{kg}^{-1}$, respectively) was investigated. The 100 wt % FCC binders were also prepared for comparison purposes. After establishing the optimum FCC percentage (30 wt %), the influence of different SiO_2 concentrations (2.91 to $7.28 \text{ mol}\cdot\text{kg}^{-1}$ of water) on the mechanical properties of the developed systems was analyzed. As the sodium concentration remained constant throughout the study (Table 1), the $\text{SiO}_2/\text{Na}_2\text{O}$ molar ratios varied from 0.78 to 1.94. Given that, as explained by Mellado et al. [11], the vast majority of the CO_2 emissions in alkali-activated systems are attributed to commercial waterglass, the objective of this part of the study was to minimize the emissions of the newly developed binders, which contributes to improve their sustainability. After establishing the optimum silica concentration ($4.37 \text{ mol}\cdot\text{kg}^{-1}$, which gave good compressive strength results with the lowest silica content), the influence of FCC additions on the alkali-activated CSW systems was explored again. This provided information on the mechanical properties and microstructure developed with both silica concentrations (initial and optimized).

Designation of pastes and mortars (Table 1) was defined according to their FCC content and SiO_2 concentration in such a way that '10/7.28' corresponded to a sample containing 10 wt % FCC, activated with a solution containing 7.28 mols of silica per kg of water (concentrations in molality terms). Mix proportions were adopted from previous studies [18] where compressive strength results higher than 25 MPa were achieved in alkali-activated CSW mortars containing 4.5 wt % $\text{Ca}(\text{OH})_2$, activated with solutions prepared with $3.75 \text{ mol}\cdot\text{kg}^{-1}$ of Na_2O and $7.28 \text{ mol}\cdot\text{kg}^{-1}$ of SiO_2 . As previously reported in [32], where porcelain stoneware tiles were used as a precursor (material that behaved similarly to CSW when alkali-activated), addition of $\text{Ca}(\text{OH})_2$ was essential to successfully activate this ceramic waste, and strongly influenced the workability and setting time of the developed mortars. Based on both previous studies [18,32], 4 wt % $\text{Ca}(\text{OH})_2$ was added to the CSW samples (no calcium hydroxide was used in the 100 wt % FCC systems). Pastes and mortars were cured following the conditions summarized in Table 1: in a temperature- and humidity- controlled chamber at 20°C with 95% relative humidity (RH) for 28 and 90 days; and in a water bath at 65°C for 7 days, inside a sealed box, with 100% RH.

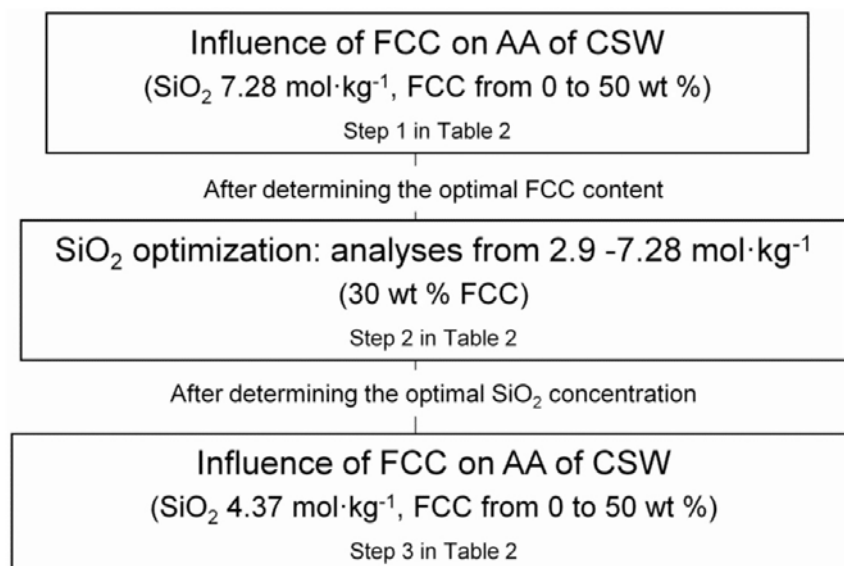


Figure 1. Experimental process of the influence of the FCC and SiO_2 concentrations on the alkali activation of CSW.

Table 1. Designation, mix proportions, ratios and curing conditions used to develop the CSW/FCC alkali-activated binders.

Step	Designation	FCC wt %	w/b ^a	Activating Solution			Na ₂ O mol·kg _{binder} ⁻¹	SiO ₂ mol·kg _{binder} ⁻¹	Ca(OH) ₂ ^b wt %	Curing Conditions
				Na ₂ O mol·kg ⁻¹	SiO ₂ mol·kg ⁻¹	SiO ₂ /Na ₂ O Molar Ratio				
1	0/7.28	0								
	10/7.28	10								
	20/7.28	20								
	30/7.28	30			7.28	1.94	1.69	3.28	4	
	40/7.28	40								
	50/7.28	50								
	100/7.28	100						0		
2	30/2.91				2.91	0.78		1.31		
	30/3.64				3.64	0.97		1.64		
	30/4.37	30	0.45	3.75	4.37	1.16	1.69	1.97	4	
	30/5.82				5.82	1.55		2.62		
	30/7.28				7.28	1.94		3.28		
3	0/4.37	0								
	10/4.37	10								
	20/4.37	20								
	30/4.37	30			4.37	1.16	1.69	1.97	4	
	40/4.37	40								
	50/4.37	50								
	100/4.37	100						0		

^a Water (w), composed of that provided by the sodium silicate solution plus tap water directly added to the activating solution; binder (b), composed of CSW and the different FCC contents. ^b Ca(OH)₂ used as an addition to the binder in the pastes and mortars that contained CSW.

2.3. Sample Preparation and Characterization

CSW powder and $\text{Ca}(\text{OH})_2$ were dry-mixed and having homogenized the mixture, the corresponding amount of FCC was added, and the mixing process continued until a homogeneous blend was obtained. The activating solution (formed by NaOH, waterglass and water) was then mixed with the blended powder until the paste was uniform. Pastes and mortars were prepared with a water/binder ratio (w/b) of 0.45: water was composed of that contained in the sodium silicate solution, plus tap water, and the binder was formed by CSW and its partial substitution with FCC ($\text{Ca}(\text{OH})_2$ was used as an addition). Mortar samples of 40 mm \times 40 mm \times 160 mm were prepared using siliceous aggregates with a fineness modulus of 4.3, and a binder/sand weight ratio of 1:3. The prismatic samples were wrapped with plastic film until they reached the testing age to prevent efflorescence formation and maintain moisture during the curing process.

The particle size distribution of the FCC and CSW milled powder was determined by laser diffraction in a Mastersizer 2000 by Malvern Instruments (Malvern, United Kingdom). Powder was stirred in water at 1200 rpm and ultrasounds were applied for 1 min to disperse possible particle agglomerations. The amorphous content of the CSW and FCC waste was determined according to Standard UNE EN 196-2:2006, and their chemical composition was determined by X-ray fluorescence (XRF) in a Philips Magix Pro spectrometer. Microstructure evolution was investigated in the pastes blended with 0 wt %–50 wt % FCC, activated with SiO_2 concentrations of 4.37 and 7.28 mol \cdot kg $^{-1}$, and cured at 65 °C for 7 days and at 20 °C for 28 days. The 100 wt % FCC pastes were also prepared as a reference. X-ray diffraction (XRD) analyses of raw materials and pastes were run in a Bruker AXS D8 Advance (Billerica, MA, USA) by taking Cu K α radiation, from 10 to 70 2 θ degrees, at 20 mA and 40 kV, using an angle step of 0.02 and a 2-s accumulation time. The FESEM analyses were run in an FESEM ULTRA 55, by ZEISS (Oberkochen, Germany). The paste samples were coated with carbon and images were taken at 2 kV. The tests were run in a Mettler Toledo TGA 850 thermobalance from 35 to 600 °C, at a heating rate of 10 °C/min, in a nitrogen atmosphere at a flow gas rate of 75 mL \cdot min $^{-1}$. Aluminum-sealed crucibles (100- μ L volume) with a pinholed lid were used. The compressive strength tests were performed in mortars according to Standard UNE EN 196-1.

3. Results and Discussion

3.1. Properties of Raw Materials

Figure 2 shows the morphology of the CSW particles (crushed and milled) and FCC. As observed, the crushed CSW particles are composed of a glaze covering and a ceramic body (Figure 2a). Both parts homogenized after particle size diminished during the milling process, and the field emission scanning electron microscopy images denote dense irregular particles with a smooth surface (Figure 2b). The FCC particles (Figure 2c) exhibited higher porosity and a smaller particle size compared with the milled CSW, which conferred them a larger specific surface.

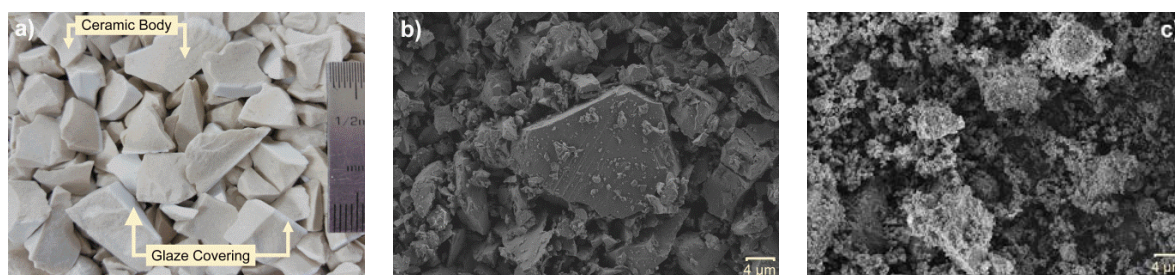


Figure 2. Images of the materials used as a precursor: (a) Crushed CSW; (b) Milled CSW; (c) As-received FCC.

The CSW particles presented a mean diameter of 31.24 μm , with 10 vol % of particles under 2.92 μm , 50 vol % under 22.38 μm , and 90 vol % under 73.32 μm (d_{10} , d_{50} and d_{90} values, respectively). In agreement with the FESEM micrographs, the FCC powder had a smaller particle size, with a mean diameter of d_{10} , d_{50} and d_{90} of 17.12, 1.10, 9.61 and 45.12 μm , respectively.

The XRD spectra of the raw materials used as a precursor in the alkali-activated systems are presented in Figure 3. The main crystalline phases identified in the ceramic material were quartz (Q, SiO_2 , PDFcard331161) and mullite (M, $\text{Al}_6\text{Si}_2\text{O}_{13}$, PDFcard150776), and small amounts of calcium feldspar anorthite (A, $\text{CaAl}_2\text{Si}_2\text{O}_8$, PDFcard411486) were also distinguished. The signals attributed to quartz and mullite also arose in the FCC spectra, together with those assigned to sodium feldspar Albite (B, $\text{NaAlSi}_3\text{O}_8$, PDFcard200554) and sodium-faujasite (F, $\text{Na}_2\text{Al}_2\text{Si}_4\text{O}_{12}\cdot 8\text{H}_2\text{O}$, PDFcard391380). Both materials exhibited a deviation from the baseline (from 17 to 32 2θ degrees), which denotes the presence of amorphous phases in the waste materials. According to Rodríguez et al. [29], the amorphous phases in FCC are formed by the partial destruction of zeolites during the catalytic cracking process. Zeolitic phases have also been distinguished by Trochez et al. [21], Rodríguez et al. [29] and Tashima et al. [28], who used FCC as a precursor to produce alkali-activated binders. As described by Rodríguez et al. [29], FCC may be considered to be zeolitic phases bound by an aluminosilicate matrix.

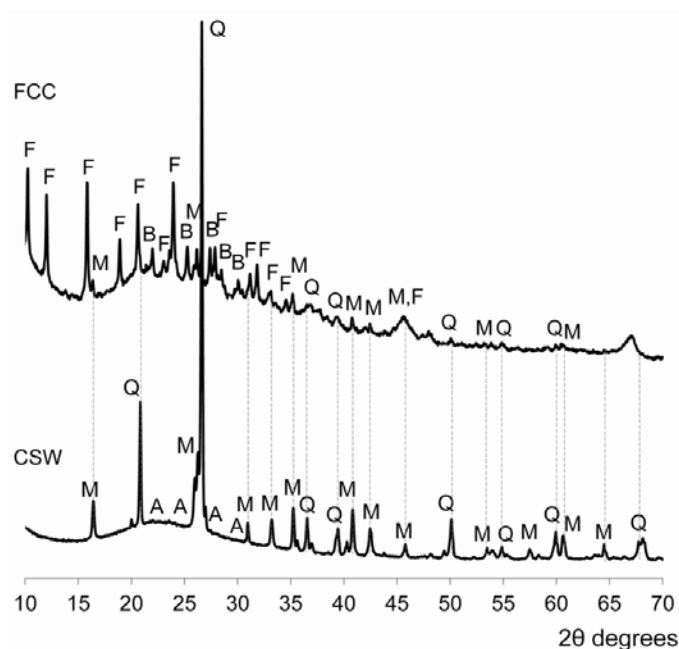


Figure 3. Mineralogical composition of the FCC and CSW raw materials. Quartz (Q, SiO_2); Mullite (M, $\text{Al}_6\text{Si}_2\text{O}_{13}$); Anorthite (A, $\text{CaAl}_2\text{Si}_2\text{O}_8$); Albite (B, $\text{NaAlSi}_3\text{O}_8$); sodium-faujasite (F, $\text{Na}_2\text{Al}_2\text{Si}_4\text{O}_{12}\cdot 8\text{H}_2\text{O}$).

Table 2 shows the chemical composition of FCC and CSW. As observed, both materials contained large amounts of SiO_2 and Al_2O_3 (97.02 wt % and 89.06 wt % the sum for FCC and CSW, respectively), and the percentage of alumina was significantly higher for FCC. CSW exhibited a SiO_2 -to- Al_2O_3 mass ratio of 2.79, and this ratio came close to 1 for FCC. Similar Al_2O_3 and SiO_2 contents have been previously reported by Rodríguez et al. [29] for FCC (48.40 wt %, and 46.94 wt %, respectively), while slightly lower Al_2O_3 values (41.57 wt % and 48.09 wt %, for Al_2O_3 and SiO_2 , respectively) have been recorded by Trochez et al. [21] for an FCC obtained from a Colombian petroleum company (both FCC were also alkali-activated to produce binders). In the study by Pacewska et al. [26], the Al_2O_3 and SiO_2 contents of two different FCC varied within the 38%–41% range and the 50%–54% range, respectively, which led to a slightly higher $\text{SiO}_2/\text{Al}_2\text{O}_3$ mass ratio (1.33).

Oxides other than alumina and silica (CaO, Fe₂O₃, K₂O or Na₂O) in the ceramic material were attributed to their presence on the clay used to manufacture the CSW units since, as observed by Pacheco-Torgal and Jalali [33], the chemical composition of the ceramic products is similar to that of the original clays. The amorphous content of the CSW and FCC wastes was respectively 45.6% and 88.3%.

Table 2. Chemical composition of the FCC and CSW wastes (wt %).

	Al ₂ O ₃	SiO ₂	CaO	Fe ₂ O ₃	K ₂ O	Na ₂ O	P ₂ O ₅	Other	LOI *
FCC	49.26	47.76	0.11	0.60	0.02	0.31	0.01	1.42	0.51
CSW	23.60	66.00	1.20	1.30	2.80	2.40	0.50	2.00	0.20

* Determined at 950 °C.

3.2. Compressive Strength

Figure 4 shows the compressive strength results of the alkali-activated CSW/FCC blended mortars, developed with 7.28 mol·kg⁻¹ of SiO₂ and increasing amounts of FCC (0 wt %–50 wt %), cured at 65 °C for 7 days, and at 20 °C for 28 and 90 days (Step 1 of the study, according to Figure 3 and Table 1). The alkali-activated 100 wt % FCC mortars were prepared for comparison purposes. As observed, the compressive strength values significantly improved with FCC addition as up to 70 MPa were achieved in the mortars containing 50 wt % FCC cured at room temperature for 90 days. Both waste materials exhibited a synergetic effect, so that the mechanical properties given by the blended systems were higher than those obtained when only one waste was used as a precursor (100 wt % CSW or FCC mortars). These results agree with the previous findings of Fernández-Jiménez et al. [34] who, after exploring the influence of reactive alumina on alkali-activated fly ashes, concluded that the ashes which best performed when activated were those with large amounts of reactive SiO₂ and Al₂O₃ (determined as a mass percentage) and with Si/Al reactive atomic ratios below 2. Since FCC is an Al₂O₃-rich residue with a high percentage of soluble fraction (88.3% amorphous content), the FCC additions in the alkali-activated CSW mortars provided reactive silica and alumina and lowered the SiO₂/Al₂O₃ ratio of the blended system (originally 2.79, and 1 for the CSW and FCC precursors, respectively).

The CSW mortars containing up to 20 wt % FCC obtained better compressive strength results when cured at 65 °C than at room temperature, and this tendency reversed with further FCC additions. This behavior was attributed to the fact that thermal energy was required to activate the chemical reactions in 100 wt % and 90 wt % CSW mortars. Thus, the beneficial effect produced by FCC in the CSW alkali-activated systems was especially important at room temperature since the strength values of the 100 wt % CSW mortars cured at 20 °C for 28 days increased from 3.6 to 26.6 MPa and to 39.5 MPa with the 20 wt % and 30 wt % FCC additions, respectively. These results confirm the beneficial influence of FCC in the alkali-activated CSW binders and greatly extend their application field. Similar results have been previously reported in [17], where addition of Ca(OH)₂, PC or CAC significantly improved the strength of the alkali-activated CSW binders: up to 78.6 MPa and 66.3 MPa were achieved in the mortars blended with 20 wt % CAC and 15 wt % PC, respectively (cured at 65 °C for 7 days). However, the practical benefit of FCC compared with the PC or CAC additions, which have a high negative environmental impact, lies in an industrial by-product being reused.

The low strength values exhibited by the 100 wt % FCC mortars (lower than 20 MPa) significantly differed from the optimum ones previously reported by Tashima et al. [28]. These authors obtained up to 68.3 MPa in mortars cured at 65 °C for 3 days, prepared with a water/FCC ratio of 0.60, and activated with 10 mol·Kg⁻¹ of Na and a SiO₂/Na₂O molar ratio of 1.17. Trochez et al. [21] have also reported compressive strength values within the 2.5 to 67 MPa range in alkali-activated FCC pastes cured at room temperature for 7 days. The best results were obtained with a SiO₂/Na₂O molar ratio of 0.72 (activating solution), and overall SiO₂/Al₂O₃ and Na₂O/Si₂O ratios of 2.4 and 0.25, respectively. The differences with the strength values obtained herein for the 100 wt % FCC mortars were attributed to the different mix proportions used (7.5 mol·Kg⁻¹ of Na and a SiO₂/Na₂O molar ratio of 1.94 in Step 1 of the study) compared with the optimum solutions reported by Tashima et al. [27,28]

and Trochez et al. [21]. The cited works [21,27,28] observed that excess silicates in the system (high $\text{SiO}_2/\text{Na}_2\text{O}$ ratios) resulted in reduced strength. Similarly, as explained by Rodríguez et al. [29] and Trochez et al. [21], highly alkaline solutions are required to dissolve the AlO_4^- species in the FCC precursor since an insufficient presence of alkalis retards the dissolution of zeolites and leads to a larger amount of unreacted FCC which, consequently, reduces binder formation.

FCC 30 wt % was established as the optimum percentage in Stage 1 of the study since the compressive strength exhibited by this mortar (40 MPa after 28 curing days at room temperature) was considered high enough to allow its use in general construction applications. Moreover, the improvement of strength observed with 10 wt % increments of FCC progressively reduced, so that compressive strength results improved 20.1 MPa, 17.4 MPa, 9.2 MPa and 3.6 MPa when increasing the FCC content 10 wt %–20 wt %, 20 wt %–30 wt %, 30 wt %–40 wt % and 40 wt %–50 wt %, respectively. Since, as previously explained in the Introduction, waterglass is the component with the highest environmental impact on alkali-activated binders [11], the purpose of the second part of this study was to lower the SiO_2 concentration to improve the developed mortars' sustainability. The compressive strength of the mortars blended with 30 wt % FCC, prepared with silica concentrations ranging from 2.91 to 7.28 $\text{mol}\cdot\text{kg}^{-1}$ and cured at 65 °C for 7 days, is plotted in Figure 5. As observed, the strength results progressively increased with the SiO_2 concentration, and similar values were recorded in the mortars prepared with the largest amounts of silica (5.82 and 7.28 $\text{mol}\cdot\text{kg}^{-1}$). Tashima et al. [27] have also observed a progressive increase in compressive strength with the silica content in FCC mortars alkali-activated with 10 $\text{mol}\cdot\text{kg}^{-1}$ of sodium. In their study [27], optimum results (≈ 70 MPa after 3 curing days at 65 °C) were obtained with 1.58 mols of SiO_2 (equivalent to 3.51 $\text{mol}\cdot\text{kg}_{\text{binder}}^{-1}$ which, as reported in Table 1, comes close to the 3.28 $\text{mol}\cdot\text{kg}_{\text{binder}}^{-1}$ that corresponds to 7.28 $\text{mol}\cdot\text{kg}^{-1}$ of silica in the activating solution), and decreased with further additions (≈ 60 MPa with 1.97 mols of SiO_2 , equivalent to 4.38 $\text{mol}\cdot\text{kg}_{\text{binder}}^{-1}$).

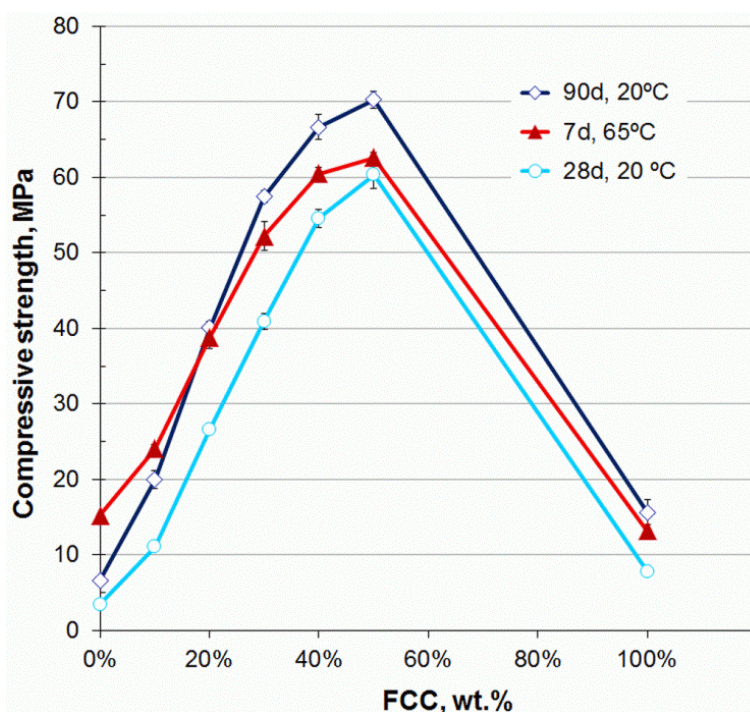


Figure 4. Evolution of compressive strength with the FCC content in the alkali-activated CSW mortars prepared with 7.28 $\text{mol}\cdot\text{kg}^{-1}$ SiO_2 activating solutions, cured at 65 °C for 7 days and at 20 °C for 28 and 90 days.

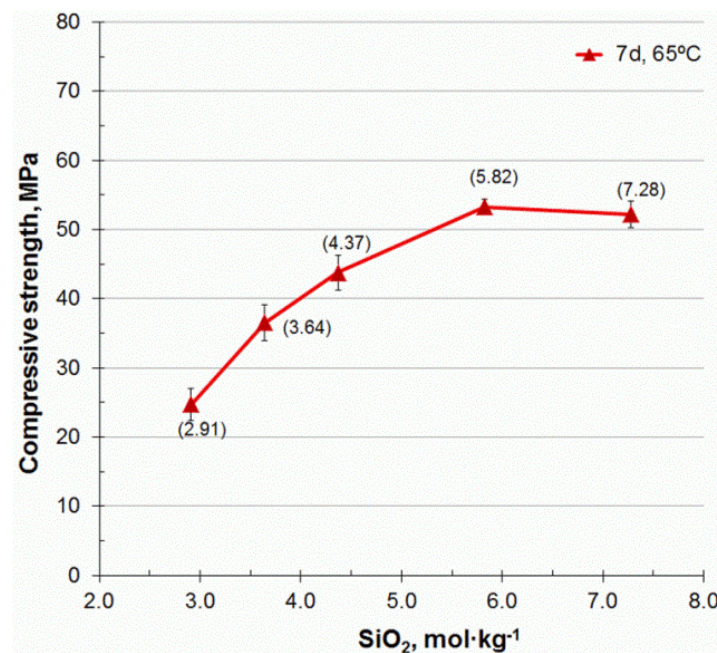


Figure 5. Compressive strength evolution with the SiO₂ concentration (indicated in parentheses) in the alkali-activated CSW mortars containing 30 wt % FCC cured at 65 °C for 7 days.

A silica concentration of 4.37 mol·kg⁻¹ which, as shown in Figure 5, provided strength results that came close to 44 MPa, was selected for the final study stage. This compressive strength was still significantly higher than that recorded for the 100 wt % CSW mortar activated with 7.28 mol·kg⁻¹ of SiO₂, which yielded 15.3 MPa after 7 days at 65 °C (Figure 4). Silica content (added as waterglass) reduced from 3.28 mol·kg_{binder}⁻¹ to 1.97 SiO₂ mol·kg_{binder}⁻¹ (as reported in Table 1), which certainly contributed to improve the developed mortars' sustainability. The compressive strength evolution of the CSW mortars blended with 0 wt %–50 wt % FCC, alkali-activated with 4.37 and 7.28 mol·kg⁻¹ silica concentrations, cured at 65 °C for 7 days, and at 20 °C for 28 and 90 days, is plotted in Figure 6. As observed, CSW blended mortars exhibited better mechanical properties with the highest silica concentration, no matter what the FCC content, and these differences were more noticeable at higher temperatures (65 °C) or for longer curing times (90 days). Nevertheless, the strength values recorded after 28 days at room temperature with 4.37 mol·kg⁻¹ of SiO₂ and 30 wt % (or higher) FCC contents were high enough to allow the use of these binders in common construction uses. While waterglass content lowered by 40% when using 4.37 mol·kg⁻¹ of SiO₂, loss of strength between the high- and low-silica mortars prepared with the same FCC contents reduced by maximum 21.37% and 27.95% after 28 and 90 curing days, respectively (strength loss calculated in the mortars containing 20 wt %–50 wt % FCC). As the better mechanical properties provided by the higher silica concentrations would allow higher strength concrete to be developed, reducing the section of the construction elements or applying loads with shorter curing times, the alkali-activated binders prepared with 7.28 mol·kg⁻¹ silica in the activating solution would be recommended for special applications in which higher mechanical properties are required.

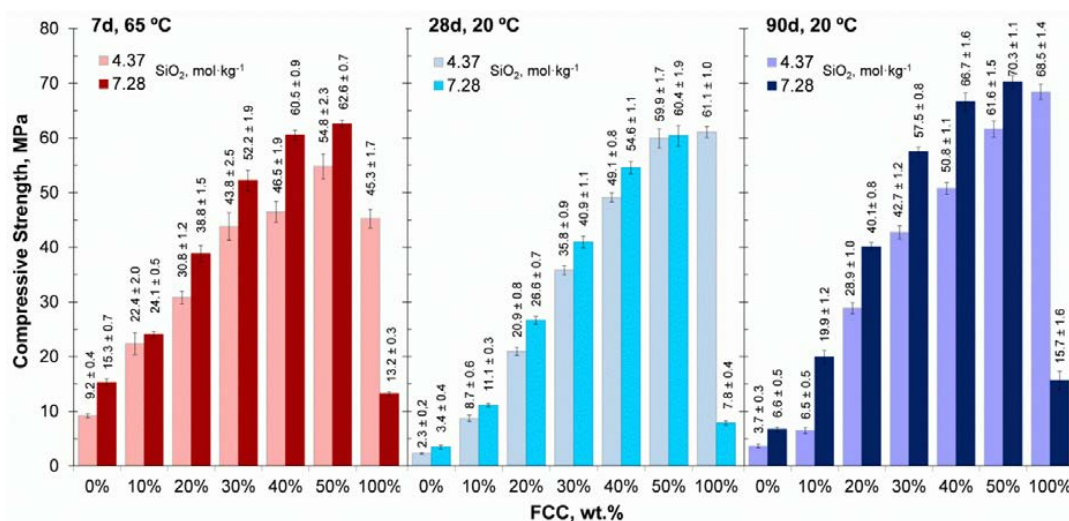


Figure 6. Compressive strength of the alkali-activated CSW mortars cured at 65 °C for 7 days, and at 20 °C for 28 and 90 days. Influence of the FCC contents and SiO₂ concentrations in the activating solution.

3.3. X-ray Diffraction (XRD)

The XRD spectra for the CSW/FCC blended pastes, alkali-activated with solutions containing 4.37 and 7.28 mol·kg⁻¹ of SiO₂, are reported in Figures 7 and 8. The spectra of the pastes cured at 20 °C for 28 days are shown in Figure 7, while those of the pastes cured at 65 °C for 7 days are presented in Figure 8. Quartz and mullite, both previously identified in the raw CSW and FCC materials, were also detected in all the activated pastes. This denotes that these crystalline stable phases did not significantly participate in the alkali-activation process. Signals attributed to the calcium feldspar anorthite were easily distinguished in the 100 wt % CSW activated paste and that blended with 10 wt % FCC, while the intensity of the peaks assigned to albite progressively increased with FCC content. Signals due to sodium-faujasite, which arose in the FCC spectra (Figure 3), were not distinguished in the activated pastes. This suggests that this zeolite was dissolved by the activating solution to provide Al and Si, which promoted the formation of an aluminosilicate-type binding gel. These results well agree with those previously reported by Rodríguez et al. [29], who also identified crystalline mullite and quartz, but neither observed the faujasite-type zeolite after the activation of FCC, no matter what activating conditions were used.

A displacement of the baseline toward higher 2θ angles (from 17 to 32 2θ degrees in the raw materials to 25–35 2θ degrees in the activated pastes) was observed with increasing FCC additions. Trochez et al. [21] and Tashima et al. [28] have also reported a deviation from the baseline in FCC activated pastes, which was attributed to the formation of a new amorphous aluminosilicate-type gel during the alkali-activation process. No signals due to Ca(OH)₂, which was added to all the CSW pastes, were distinguished in the XRD patterns of the activated pastes, which suggests that calcium hydroxide is consumed during the activation process. These results fall in line with the previous findings reported by Reig et al. [17,32], who did not distinguish Ca(OH)₂ after the activation of either porcelain stoneware tiles [32] or CSW [17].

No significant amounts of new crystalline phases were identified by the XRD analyses. Sodium carbonate Natron (N, Na₂CO₃·10H₂O, PDFcard150800) formed in some of the activated pastes, mainly those prepared using a single raw material as a precursor (100% CSW or 100% FCC). This sodium carbonate has been previously identified in CSW alkali-activated pastes containing up to 8 wt % Ca(OH)₂ [17], and in similar alkali-activated ceramic materials, such as porcelain stoneware tiles (blended with 2 wt %–5 wt % calcium hydroxide) [32]. Sodium carbonates have also been distinguished by Tashima et al. [28] in alkali-activated FCC pastes, and have been attributed to sample carbonation,

or to the presence of unreacted reagents. The zeolite natrolite (T, $\text{Na}_2\text{Al}_2\text{Si}_3\text{O}_{10}\cdot 2\text{H}_2\text{O}$, PDFcard 200759) formed in the 100 wt % FCC pastes activated at room temperature with $4.37 \text{ mol}\cdot\text{kg}^{-1}$ of SiO_2 (Figure 7a). Peaks attributed to other zeolites were observed only in the pastes cured at 65°C and developed with 100 wt % or 50 wt % FCC (Figure 8). More specifically, of the pastes cured at 65°C , zeolite A (Z, $\text{Na}_2\text{Al}_2\text{Si}_{1.85}\text{O}_7\cdot 7.5\text{H}_2\text{O}$, PDFcard380241) arose in the 100 wt % FCC pastes (regardless of the silica concentration), and that blended with 50 wt % FCC and activated with $7.28 \text{ mol}\cdot\text{kg}^{-1}$ of silica. Zeolites Herschelite (H, $\text{Na AlSi}_2\text{O}_6\cdot 3\text{H}_2\text{O}$, PDFcard191178) and Rh0 (R, formed by eight sodalite units, $\text{Al}_{12}\text{H}_{12}\text{Si}_{36}\text{O}_{96}$, PDFcard270015) were identified in the 100 wt % FCC pastes activated with 7.28 and $4.37 \text{ mol}\cdot\text{kg}^{-1}$ SiO_2 , respectively. Different zeolite type phases have also been distinguished by Trochez et al. [21] in alkali-activated FCC systems. It is important to highlight that zeolites formation was not favored in the systems with higher CSW contents (0 wt %–30 wt % FCC), which denotes the high metastability of the formed amorphous binding gel.

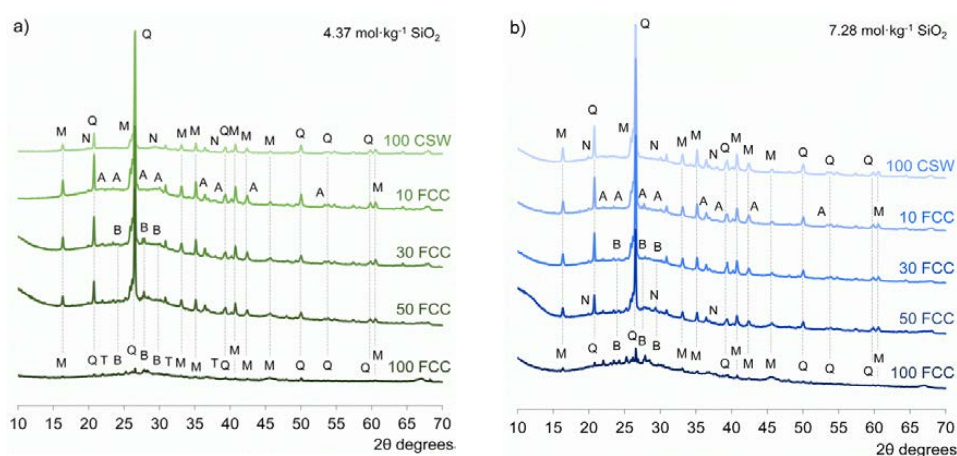


Figure 7. XRD spectra for the CSW/FCC blended pastes containing different amounts of FCC, cured at 20°C for 28 days, and alkali-activated with solutions prepared with SiO_2 concentrations of: (a) $4.37 \text{ mol}\cdot\text{kg}^{-1}$; (b) $7.28 \text{ mol}\cdot\text{kg}^{-1}$. Quartz (Q, SiO_2); Mullite (M, $\text{Al}_6\text{Si}_2\text{O}_{13}$); Anorthite (A, $\text{CaAl}_2\text{Si}_2\text{O}_8$); Albite (B, $\text{NaAlSi}_3\text{O}_8$); Natron (N, $\text{Na}_2\text{CO}_3\cdot 10\text{H}_2\text{O}$); Natrolite (T, $\text{Na}_2\text{Al}_2\text{Si}_3\text{O}_{10}\cdot 2\text{H}_2\text{O}$).

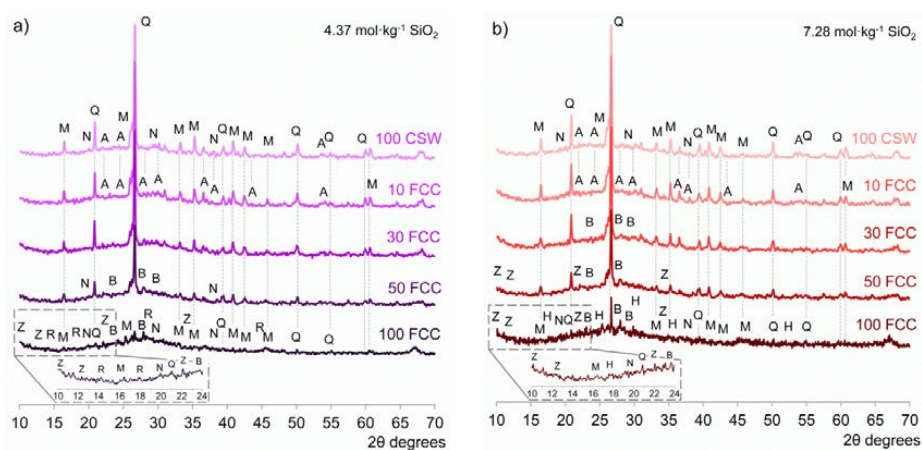


Figure 8. XRD spectra for the CSW/FCC blended pastes containing different amounts of FCC, cured at 65°C for 7 days, alkali-activated with solutions prepared with SiO_2 concentrations of: (a) $4.37 \text{ mol}\cdot\text{kg}^{-1}$; (b) $7.28 \text{ mol}\cdot\text{kg}^{-1}$. Quartz (Q, SiO_2); Mullite (M, $\text{Al}_6\text{Si}_2\text{O}_{13}$); Anorthite (A, $\text{CaAl}_2\text{Si}_2\text{O}_8$); Albite (B, $\text{NaAlSi}_3\text{O}_8$); Natron (N, $\text{Na}_2\text{CO}_3\cdot 10\text{H}_2\text{O}$); Herschelite (H, $\text{Na AlSi}_2\text{O}_6\cdot 3\text{H}_2\text{O}$); Zeolite A (Z; $\text{Na}_2\text{Al}_2\text{Si}_{1.85}\text{O}_7\cdot 7.5\text{H}_2\text{O}$); Zeolite Rh0 (R, $\text{Al}_{12}\text{H}_{12}\text{Si}_{36}\text{O}_{96}$).

3.4. Thermal Analysis

Figure 9 shows the curves for the CSW/FCC blended pastes prepared with 0 wt %, 10 wt %, 30 wt % and 50 wt % FCC, activated with SiO_2 concentrations of 4.37 and 7.28 mol·kg⁻¹ and cured at 20 °C for 28 days and at 65 °C for 7 days. 100 wt % FCC pastes were also prepared for comparison purposes. The total mass loss recorded during the tests is indicated as a percentage.

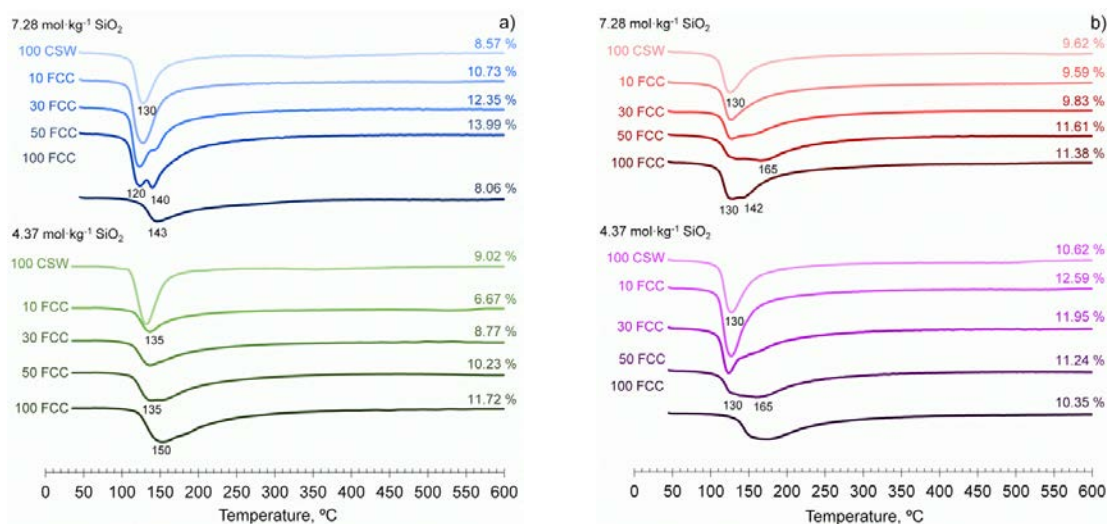


Figure 9. Differential curves for the CSW and FCC blends, activated with solutions prepared with SiO_2 concentrations of 4.37 and 7.28 mol·kg⁻¹, cured at: (a) 20 °C for 28 days; (b) 65 °C for 7 days. Total mass loss indicated as a percentage.

All the DTG curves presented a single band from 100 to 200 °C which, according to [35], typically arises due to the dehydration of the newly-formed N-A-S-H or (N,C)-A-S-H gels. The TG analyses were unable to confirm the presence of zeolitic phases, previously identified by XRD, since the signal originated by the dehydration of zeolites also appears within this temperature range (60–160 °C) [35]. While the 100 wt % CSW activated pastes exhibited a narrower and defined peak at 130 °C, it broadened with increasing FCC contents, which suggests a change in the binding gel structure. Total loss of mass generally increased with FCC addition, and was greater for the blended pastes than for those prepared with a single raw material (100 wt % CSW or 100 wt % FCC). Mass loss results well agree with the compressive strength evolution reported in Figure 6, and are attributed to greater binding gel formation, whose dehydration resulted in a greater loss of water and/or OH groups with increasing FCC contents.

No signals attributed to Ca(OH)_2 (520–580 °C) [32] were distinguished in any of the CSW activated pastes, which confirms the results previously obtained by XRD, where no peaks assigned to calcium hydroxide arose after the activation process. This indicates that calcium is consumed during the activation process and, as previously described in [32], it may displace sodium and act as a charge-balancing ion to lead to (C,N)-A-S-H gels. The TG analyses were unable to confirm the presence of natron, whose signals arose in some XRD spectra, because, according to Hidalgo et al. [36], the characteristic bands of carbonates arise within the 625–875 °C range.

3.5. Field Mission Scanning Electron Microscopy (FESEM)

FESEM micrographs of the pastes prepared with 100 wt % CSW, 30 wt % FCC and 100 wt % FCC, alkali-activated with solutions containing 4.37 and 7.28 mol·kg⁻¹ of SiO_2 , are shown in Figures 10–13. While the microstructure of the pastes cured at room temperature for 28 days is shown in Figures 10 and 11 (at lower and higher magnifications, respectively), that of the pastes cured at 65 °C for 7 days is presented in Figures 12 and 13. The compressive strength results obtained for

the 100 wt % CSW alkali-activated mortars cured at room temperature (lower than 3.5 MPa after 28 curing days) agree with the characteristics of the pastes, which were weak and soft. As observed in Figures 10 and 11, the morphology of the 100 wt % CSW pastes activated at 20 °C differed from that typically formed in N-A-S-H/(C,N)-A-S-H gels (30 wt % or 100 wt % FCC micrographs). The low mechanical properties and the morphology of these pastes suggest that no typical alkali-activation reactions occurred to a great extent. The 100 wt % FCC pastes activated at room temperature with the lowest silica concentration presented a dense homogeneous structure and, in consonance with the XRD spectra, where peaks attributed to the zeolitic phase natrolite were identified, microcrystals which resembled zeolitic products were distinguished (labeled as ZE in Figure 11). Although no signals due to zeolites were identified by the XRD analyses in the 30 wt % FCC paste activated at 20 °C with 7.28 mol·kg⁻¹ of SiO₂ (Figure 7b), typical zeolitic-like morphologies were observed at a higher magnification (Figure 11, labeled as ZE), which denotes that small amounts of zeolites may also form under these conditions.

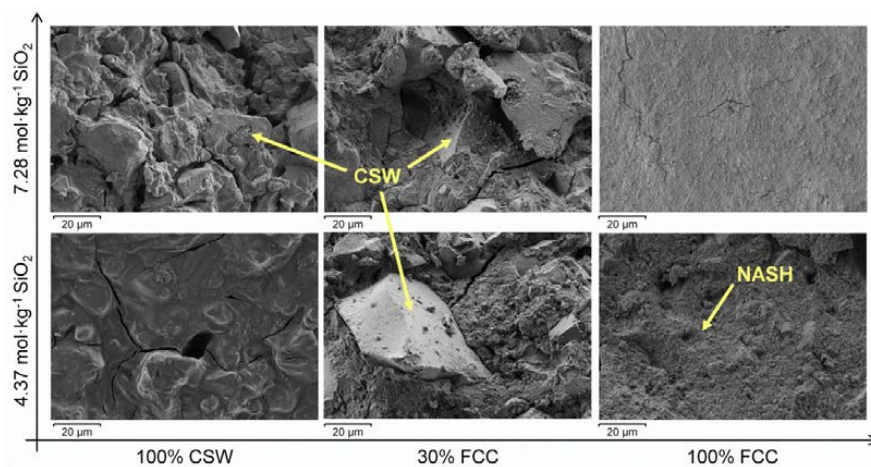


Figure 10. Field emission scanning electron images of the CSW/FCC blended pastes prepared with 100 wt % CSW, 30 wt % FCC and 100 wt % FCC, alkali-activated with solutions containing 4.37 and 7.28 mol·kg⁻¹ of SiO₂, and cured at 20 °C for 28 days. CSW: ceramic sanitary-ware unreacted particles; NASH: alkali-activated binding gel.

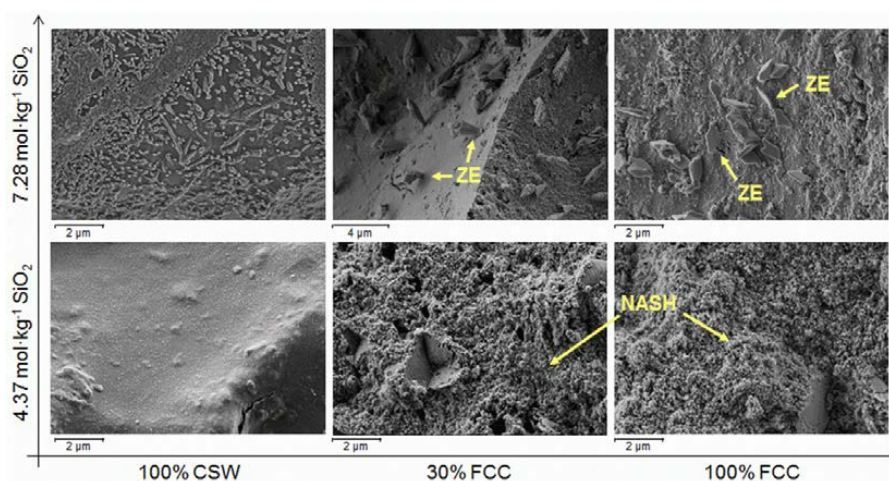


Figure 11. Field emission scanning electron images of the CSW/FCC blended pastes prepared with 100 wt % CSW, 30 wt % FCC and 100 wt % FCC, alkali-activated with solutions containing 4.37 and 7.28 mol·kg⁻¹ of SiO₂, and cured at 20 °C for 28 days. Higher magnification. NASH: alkali-activated binding gel; ZE: zeolitic phases.

As observed in Figures 12 and 13, the 100 wt % CSW paste and that containing 30 wt % FCC presented a similar microstructure after 7 curing days at 65 °C, in which unreacted CSW particles, surrounded by reaction products, can be easily distinguished. Variations in the silica concentration or the amount of FCC did not lead to significant differences in the morphology of the newly formed gel. In agreement with the compressive strength results recorded for the 100 wt % FCC mortars, which increased when activated with the 4.37 mol·kg⁻¹ of SiO₂ solutions (Figure 6), the microstructure of these pastes was denser when activated with lower SiO₂ concentrations. Sodium carbonate salt (natron) was also observed with the highest SiO₂ contents (identified with letter N in Figures 12 and 13), which denoted excess alkalis in the activating solution. These carbonates have also been previously distinguished in alkali-activated porcelain stoneware tiles [32]. Although zeolite A, which cubic morphology previously observed Ozer and Soyer-Uzun in alkali-activated metakaolin [37], was identified by XRD tests in the 100 wt % FCC pastes cured at 65 °C, it could not be clearly distinguished by the FESEM analyses.

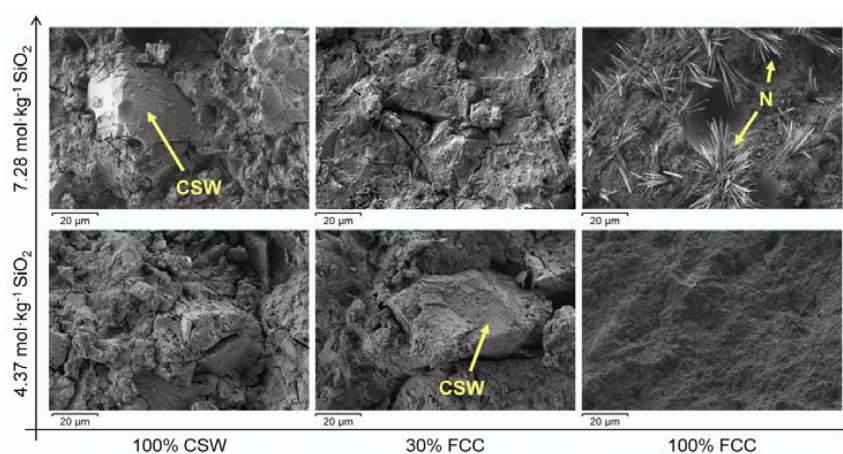


Figure 12. Field emission scanning electron images of the CSW/FCC blended pastes prepared with 100 wt % CSW, 30 wt % FCC and 100 wt % FCC, alkali-activated with solutions containing 4.37 and 7.28 mol·kg⁻¹ of SiO₂, and cured at 65 °C for 7 days. CSW: ceramic sanitary-ware unreacted particles; N: sodium carbonate Natron.

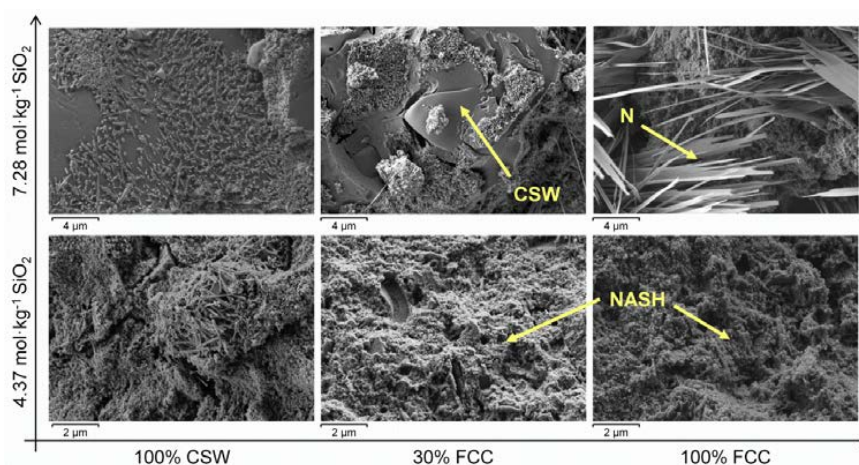


Figure 13. Field emission scanning electron images of the CSW/FCC blended pastes prepared with 100 wt % CSW, 30 wt % FCC and 100 wt % FCC, alkali-activated with solutions containing 4.37 and 7.28 mol·kg⁻¹ of SiO₂, and cured at 65 °C for 7 days. Higher magnification. CSW: ceramic sanitary-ware unreacted particles; N: sodium carbonate Natron; NASH: alkali-activated binding gel.

4. Conclusions

The influence of FCC additions (0 wt %–50 wt %) and SiO₂ concentration on the microstructure and compressive strength of alkali-activated ceramic sanitary-ware (CSW) was assessed. The following conclusions were drawn from the results obtained in this research:

- The mechanical properties of alkali-activated CSW binders significantly improved with FCC content. Strength values close to 40 MPa were obtained in the mortars blended with 20 wt % FCC cured at 65 °C for 7 days, and in those that contained 30 wt % FCC, cured at room temperature for 28 days. The compressive strength of these mortars was still higher than 30 MPa when the SiO₂ concentration was lowered from 7.28 to 4.37 mol·kg⁻¹.
- The CSW/FCC binders exhibited a wide range of mechanical properties (up to 60.4 MPa after 28 curing days at 20 °C), which varied depending on the FCC replacing percentage and the silica content in the activating solution. Bigger FCC amounts or higher silica concentrations could be used for special applications, where high strength binders or the use of construction elements in shorter periods are required.
- No significant amounts of new crystalline phases were identified in the alkali-activated CSW/FCC blended systems, where the main reaction product formed was a N-A-S-H/(C,N)-A-S-H binding gel. Zeolites were easily distinguished only in alkali-activated pastes developed with 50 wt % or 100 wt % FCC.

A general conclusion is that the partial substitution of CSW by FCC significantly improved the behavior of CSW as a precursor in alkali-activated binders. FCC additions improved the system's mechanical properties and allowed activating CSW at room temperature. However, in order to confirm and totally embrace this reutilization and valorization possibility, further studies on the durability of the developed CSW/FCC-blended systems are required.

Acknowledgments: The authors would like to thank the Spanish Ministry of Science and Innovation for supporting this research through Project APLIGEO BIA2015-70107-R, FEDER funds and the companies Ideal Standard and Omya Clariana S.A., for supplying the raw CSW and FCC materials respectively. We also wish to thank the electron Microscopy Service of the Universitat Politècnica de València.

Author Contributions: José María Monzó, María Victoria Borrachero and Jordi Payá conceived and designed the experiments; Juan Cosa and Lourdes Soriano performed the experiments; Lourdes Soriano, Lucía Reig and Juan Cosa analyzed the data; the companies Ideal Standard and Omya Clariana S.A. contributed the waste materials; Lucía Reig, Lourdes Soriano and Juan Cosa wrote the paper, which was reviewed by all the authors.

Conflicts of Interest: The authors declare no conflict of interest.

References

1. U.S. Geological Survey. Mineral Commodity Summaries 2017. 2017; pp. 44–45. Available online: <https://doi.org/10.3133/70180197> (accessed on 14 March 2018).
2. Imbabi, M.S.; Carrigan, C.; McKenna, S. Trends and developments in green cement and concrete technology. *Int. J. Sustain. Built Environ.* **2012**, *1*, 194–216. [[CrossRef](#)]
3. Shi, C.; Fernández Jiménez, A.; Palomo, A. The pursuit of an alternative to Portland cement. *Cem. Concr. Res.* **2011**, *41*, 750–763. [[CrossRef](#)]
4. Puertas, F.; García-Díaz, I.; Barba, A.; Gazulla, M.F.; Palacios, M.; Gómez, M.P. Ceramic wastes as alternative raw materials for Portland cement Clinker production. *Cem. Concr. Compos.* **2008**, *30*, 798–805. [[CrossRef](#)]
5. Puertas, F.; García-Díaz, I.; Palacios, M.; Gazulla, M.F.; Gómez, M.P.; Orduña, M. Clinkers and cements obtained from raw mix containing ceramic wastes as a raw materials. Characterization, hydration and leaching studies. *Cem. Concr. Compos.* **2010**, *32*, 175–186. [[CrossRef](#)]
6. García de Lomas, M.; Sánchez de Rojas, M.I.; Frías, M. Pozzolan reaction of a spent fluid catalytic cracking catalyst in FCC-cement mortars. *J. Therm. Anal. Calorim.* **2007**, *90*, 443–447. [[CrossRef](#)]
7. Frías, M.; Rodríguez, O.; Sánchez de Rojas, M.I.; Vilar-Cocina, E.; Rodrigues, M.; Savastano, H. Advances on the development of ternary cements elaborated with biomass ashes coming from different activation process. *Constr. Build. Mater.* **2017**, *136*, 73–80. [[CrossRef](#)]

8. Deschner, F.; Winnefeld, F.; Lothenbach, B.; Seufert, S.; Schwesing, P.; Dittrich, S.; Goetz-Neunhoeffler, F.; Neubauer, J. Hydration of Portland cement with high replacement by siliceous fly ash. *Cem. Concr. Res.* **2012**, *42*, 1389–1400. [[CrossRef](#)]
9. Ioannou, S.; Reig, L.; Paine, K.; Quillin, K. Properties of a ternary calcium sulfoaluminate-calcium sulfate-fly ash cement. *Cem. Concr. Res.* **2014**, *56*, 75–83. [[CrossRef](#)]
10. Srinivasula Reddy, M.; Dinakar, P.; Hanumantha Rao, B. A review of the influence of source material's oxide composition on the compressive strength of geopolymer concrete. *Microporous Mesoporous Mater.* **2016**, *234*, 12–23. [[CrossRef](#)]
11. Mellado, A.; Catalán, C.; Bouzón, N.; Borrachero, M.V.; Monzó, J.; Payá, J. Carbon footprint of geopolymeric mortar: Study of the contribution of the alkaline activating solution and assessment of alternative route. *RSC Adv.* **2014**, *4*, 23846–23852. [[CrossRef](#)]
12. Khan, M.Z.N.; Shaikh, F.A.; Hao, Y.; Hao, H. Synthesis of high strength ambient cured geopolymer composite by using low calcium fly ash. *Constr. Build. Mater.* **2016**, *125*, 809–820. [[CrossRef](#)]
13. Nath, P.; Sarker, P.K. Effect of GGBFS on setting, workability and early strength properties of fly ash geopolymer concrete cured in ambient condition. *Constr. Build. Mater.* **2014**, *66*, 163–171. [[CrossRef](#)]
14. Marin, C.; Araiza, J.L.R.; Manzano, A.; Avalos, J.C.R.; Perez, J.J.; Muniz, M.S.; Ventura, E.; Vorobiev, Y. Synthesis and characterization of a concrete based on metakaolin geopolymer. *Inorg. Mater.* **2009**, *45*, 1429–1432. [[CrossRef](#)]
15. Ranjbar, N.; Mehrali, M.; Behnia, A.; Alengaram, U.J.; Jumaat, M.Z. Compressive strength and microstructural analysis of fly ash/palm oil fuel ash based geopolymer mortar. *Mater. Des.* **2014**, *59*, 532–539. [[CrossRef](#)]
16. Ye, N.; Yang, J.K.; Liang, S.; Hu, Y.; Hu, J.P.; Xiao, B.; Huang, Q.F. Synthesis and strength optimization of one-part geopolymer based on red mud. *Constr. Build. Mater.* **2016**, *111*, 317–325. [[CrossRef](#)]
17. Reig, L.; Soriano, L.; Tashima, M.M.; Borrachero, M.V.; Monzó, J.; Payá, J. Influence of calcium additions on the compressive strength and microstructure of alkali-activated ceramic sanitary-ware. *J. Am. Ceram. Soc.* **2018**. [[CrossRef](#)]
18. Reig, L.; Borrachero, M.V.; Monzó, J.; Savastano, H.; Tashima, M.M.; Payá, J. Use of ceramic sanitaryware as an alternative for the development of new sustainable binders. *Key Eng. Mater.* **2016**, *668*, 172–180. [[CrossRef](#)]
19. Medina, C.; Frías, M.; Sánchez de Rojas, M.I. Microstructure and properties of recycled concretes using ceramic sanitaryware industry waste as coarse aggregate. *Constr. Build. Mater.* **2012**, *31*, 112–118. [[CrossRef](#)]
20. Baraldi, L. World sanitaryware production and exports. *Ceram. World Rev.* **2015**, *114*, 56–65.
21. Trochez, J.J.; Mejía de Gutiérrez, R.; Rivera, J.; Bernal, S.A. Synthesis of geopolymer from spent FCC: Effect of $\text{SiO}_2/\text{Al}_2\text{O}_3$ and $\text{Na}_2\text{O}/\text{SiO}_2$ molar ratios. *Mater. Constr.* **2015**, *65*, 65. [[CrossRef](#)]
22. Schreiber, R.; Yonley, G. The use of spent catalyst as a raw material substitute in cement manufacturing. *ACS Div. Petrol. Chem.* **1993**, *38*, 97–99.
23. Payá, J.; Monzó, J.; Borrachero, M.V.; Velázquez, S. Evaluation of the pozzolanic activity of fluid catalytic cracking catalyst residue (FC3R). Thermogravimetric analysis studies on FC3R-Portland cement pastes. *Cem. Concr. Res.* **2003**, *33*, 603–609. [[CrossRef](#)]
24. Pacewska, B.; Wilinska, I.; Kubissa, J. Use of spent catalyst from catalytic cracking in fluidized bed as a new concrete additive. *Therm. Acta* **1998**, *322*, 175–181. [[CrossRef](#)]
25. Chen, H.L.; Tseng, Y.S.; Hsu, K.C. Spent FCC catalyst as a pozzolanic material for high-performance mortar. *Cem. Concr. Comp.* **2004**, *26*, 657–664. [[CrossRef](#)]
26. Pacewska, B.; Nowacka, M.; Wilinska, I.; Kubissa, W.; Antonovich, V. Studies on the influence of spent FCC catalyst on hydration of calcium aluminate cements at ambient temperature. *J. Therm. Anal. Calorim.* **2011**, *105*, 129–140. [[CrossRef](#)]
27. Tashima, M.M.; Akasaki, J.L.; Castaldelli, V.N.; Soriano, L.; Monzó, J.; Payá, J.; Borrachero, M.V. New geopolymeric binder based on fluid catalytic cracking catalyst residue (FCC). *Mater. Lett.* **2012**, *80*, 50–52. [[CrossRef](#)]
28. Tashima, M.M.; Akasaki, J.L.; Melges, J.L.P.; Soriano, L.; Monzó, J.; Payá, J.; Borrachero, M.V. Alkali activated materials based on fluid catalytic cracking catalyst residue (FCC): Influence of $\text{SiO}_2/\text{Na}_2\text{O}$ and $\text{H}_2\text{O}/\text{FCC}$ ratio on mechanical strength and microstructure. *Fuel* **2013**, *108*, 833–839. [[CrossRef](#)]
29. Rodriguez, E.D.; Bernal, S.A.; Provis, J.L.; Gehman, J.D.; Monzó, J.; Payá, J. Geopolymers based on spent catalyst residue from a fluid catalytic cracking (FCC) process. *Fuel* **2013**, *109*, 493–502. [[CrossRef](#)]

30. Cheng, H.; Lin, K.L.; Cui, R.; Hwang, C.L.; Cheng, T.W.; Chang, T.M. Effect of solid-to-liquid ratios on the properties of waste catalyst-metakaolin based geopolymers. *Constr. Build. Mater.* **2015**, *88*, 74–83. [[CrossRef](#)]
31. Cheng, H.; Lin, K.L.; Cui, R.; Hwang, C.L.; Chang, Y.M.; Cheng, T.W. The effects of SiO₂/Na₂O molar ratio on the characteristics of alkali-activated waste catalyst-metakaolin based geopolymers. *Constr. Build. Mater.* **2015**, *95*, 710–720. [[CrossRef](#)]
32. Reig, L.; Soriano, L.; Borrachero, M.V.; Monzó, J.; Payá, J. Influence of the activator concentration and calcium hydroxide addition on the properties of alkali-activated porcelain stoneware. *Constr. Build. Mater.* **2014**, *63*, 214–222. [[CrossRef](#)]
33. Pacheco-Torgal, F.; Jalali, S. Reusing ceramic wastes in concrete. *Constr. Build. Mater.* **2010**, *24*, 832–838. [[CrossRef](#)]
34. Fernández-Jiménez, A.; Palomo, A.; Sobrados, I.; Sanz, J. The role played by the reactive alumina content in the alkaline activation of fly ashes. *Microporous Mesoporous Mater.* **2006**, *91*, 111–119. [[CrossRef](#)]
35. Bernal, S.A.; Gutierrez, R.M.; Provis, J.L.; Rose, V. Effect of silicate modulus and metakaolin incorporation on the carbonation of alkali silicate-activated slags. *Cem. Concr. Res.* **2010**, *40*, 898–907. [[CrossRef](#)]
36. Hidalgo, A.; García, J.L.; Alonso, M.C.; Fernández, L.; Andrade, C. Microstructure development in mixes of calcium aluminate cement with silica fume or fly ash. *J. Therm. Anal. Calorim.* **2009**, *96*, 335–345. [[CrossRef](#)]
37. Ozer, I.; Soyer-Uzun, S. Relations between the structural characteristics and compressive strength in metakaolin based geopolymers with different molar Si/Al ratios. *Ceram. Int.* **2015**, *41*, 10192–10198. [[CrossRef](#)]



© 2018 by the authors. Licensee MDPI, Basel, Switzerland. This article is an open access article distributed under the terms and conditions of the Creative Commons Attribution (CC BY) license (<http://creativecommons.org/licenses/by/4.0/>).